Anti-Arrhenius cleavage of covalent bonds in bottlebrush macromolecules on substrate

Natalia V. Lebedeva[a], Alper Nese[b], Frank C. Sun[a], Krzysztof Matyjaszewski[b], and Sergei S. Sheiko[a,1]

[a]Department of Chemistry, CB 3290, University of North Carolina, Chapel Hill, NC 27599-3290; and [b]Department of Chemistry, Carnegie Mellon University, Pittsburgh, PA 15213

Edited by Stephen L. Craig, Duke, Durham, NC, and accepted by the Editorial Board April 13, 2012 (received for review November 9, 2011)

Spontaneous degradation of bottlebrush macromolecules on aqueous substrates was monitored by atomic force microscopy. Scission of C—C covalent bonds in the brush backbone occurred due to steric repulsion between the adsorbed side chains, which generated bond tension on the order of several nano-Newtons. Unlike conventional chemical reactions, the rate of bond scission was shown to decrease with temperature. This apparent anti-Arrhenius behavior was caused by a decrease in the surface energy of the underlying substrate upon heating, which results in a corresponding decrease of bond tension in the adsorbed macromolecules. Even though the tension dropped minimally from 2.16 to 1.89 nN, this was sufficient to overpower the increase in the thermal energy (k_BT) in the Arrhenius equation. The rate constant of the bond-scission reaction was measured as a function of temperature and surface energy. Fitting the experimental data by a perturbed Morse potential $V = V_0(1 - e^{-\beta x})^2 - fx$, we determined the depth and width of the potential to be $V_0 = 141 \pm 19$ kJ/mol and $\beta^{-1} = 0.18 \pm 0.03$ Å, respectively. Whereas the V_0 value is in reasonable agreement with the activation energy $E_a = 80$–220 kJ/mol of mechanical and thermal degradation of organic polymers, it is significantly lower than the dissociation energy of a C—C bond $D_e = 350$ kJ/mol. Moreover, the force constant $K_x = 2\beta^2 V_0 = 1.45 \pm 0.36$ kN/m of a strained bottlebrush along its backbone is markedly larger than the force constant of a C—C bond $K_l = 0.44$ kN/m, which is attributed to additional stiffness due to deformation of the side chains.

mechanochemistry | molecular brushes | molecular imaging

The phenomenon of molecular "fatal adsorption," previously reported by us in 2006 (1), is a unique mechanochemical process attributed to spontaneous scission of covalent bonds in brush-like macromolecules upon their adsorption onto a substrate (Fig. 1). This molecular self-destruction is caused by remarkably strong tension of the order of several nano-Newtons, which is developed in the polymer backbone due to steric repulsion between densely grafted side chains. The crowdedness of the side chains and, hence, the backbone tension are strongly enhanced upon spreading of the side chains on a high-energy substrate. The backbone tension increases with the grafting density, the length of the side chains, and the strength of their adhesion to the substrate (2).

This unimolecular bond-scission process exhibits two distinct features. First, strong covalent bonds rupture spontaneously without applying any external force. Significant bond tension is generated within adsorbed macromolecules as they opt to rearrange their conformations in order to maximize the number of contacts between the side chains and the substrate (1,2). Second, the rate constant of the bond-scission reaction exhibits extraordinary sensitivity to minute variations of the surface energy (γ) of the underlying substrate (3). The rate constant can change by two orders of magnitude with only a 3% change in γ. In other words, the lifetime of a covalent bond may increase from 1 min to 1 h upon an incremental decrease of the substrate surface energy by *ca*. 1 mN/m, which routinely occurs in surface chemistry due to incidental variations in chemical composition, vapor pressure, and temperature. The exponential increase of the rate constant with bond tension (4–7) is vital for a wide range of applications ranging from lithography and self-healing materials to drug delivery and mechanocatalysis (8–11).

In this paper, we report a third unique feature of the adsorption-induced mechanochemistry: an anti-Arrhenius decrease of the scission rate with temperature. Observations of anti- or non-Arrhenius kinetics are rare. They are usually ascribed to an entropic contribution to the free energy of activation (e.g., in biomolecular processes that involve chain folding) (12–16). It is more typical to observe an apparent anti-Arrhenius behavior that is caused by a decrease of the equilibrium constant of a multistep reaction or changes in the surrounding environment (e.g., decrease in viscosity) (17–19). In our case, the anti-Arrhenius behavior results from a net reduction of the bond activation energy caused by the heating-induced decrease of the substrate surface energy. The goal of this paper is to demonstrate that the temperature-induced variation in surface energy can overpower the thermal energy (k_BT) and effectively slow down the bond scission. Independent control of the temperature and bond tension enabled quantitative analysis of the potential energy of a covalent bond within the bottlebrush backbone.

Results and Discussion

Our results are presented in two sections. First, we report the rate constant of bond scission as a function of temperature and bond tension. Second, we describe fitting analysis of the measured data points and evaluation of the shape of the bond potential.

Experimental Data. Every bond rupture within a brush backbone yields an extra bottlebrush molecule of a shorter length. As shown in Fig. 1, the scission processes are evidenced by two concurrent observations: (*i*) shortening of the molecular contour length and (*ii*) the corresponding increase of the number of molecules. Molecular imaging allows accurate measurements of both parameters (i.e., number-average contour length and the number of severed bonds per unit area) as a function of time under controlled temperature. Furthermore, molecular imaging allows statistical averaging for a large ensemble of molecules measured at the same time and under identical conditions (constant force). These features distinguish our experimental setup from molecular force probes that typically create a series of consecutive single-molecule extensions under a controlled loading rate (20–24).

The inherently strained macromolecules can be viewed as "molecular tensile machines" that are able autonomously to generate and control mechanical tension in their covalent bonds. In this paper, we use bottlebrush macromolecules to interrogate the

Author contributions: N.V.L., A.N., and F.C.S. performed research; K.M. contributed new reagents/analytic tools; and N.V.L. and S.S.S. wrote the paper.

The authors declare no conflict of interest.

This article is a PNAS Direct Submission. S.L.C. is a guest editor invited by the Editorial Board.

[1]To whom correspondence should be addressed. E-mail: sergei@email.unc.edu.

This article contains supporting information online at www.pnas.org/lookup/suppl/doi:10.1073/pnas.1118517109/-/DCSupplemental.

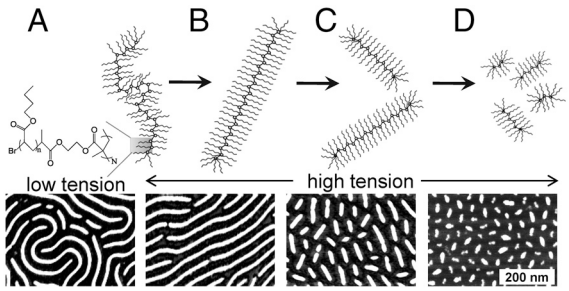

Fig. 1. Significant tension of the order of several nano-Newtons is developed in the polyacrylate backbone of molecular bottlebrushes due to steric repulsion between the densely grafted PBA side chains (*A*). This intramolecular tension leads first to nearly full extension of the backbone adopting an *all-trans* conformation (*B*) and then scission of its C—C bonds (*C*, *D*). The AFM micrographs (*Bottom*) document the random fracturing of the covalent backbone as evidenced by systematic decrease of the brush contour length.

C—C bonds in the brush backbone with respect to the effect of temperature on the scission rate. Fig. 2*A* shows molecular images of the poly(*n*-butyl acrylate) (PBA) brushes captured at different temperatures, after being adsorbed on the surface of pure water for 10 min. The molecules captured at lower temperatures are markedly shorter—i.e., they undergo faster bond scission—than molecules at higher temperatures. The decrease of the number-average contour length was measured as a function of time for different temperatures (Fig. 2*B*). To ensure the standard deviation of the mean is below 10%, at least 500 molecules were analyzed for every data point in Fig. 2*B*.

Assuming that the observed bond scission is a first-order unimolecular reaction, the time dependence of the molecular length can be written as:

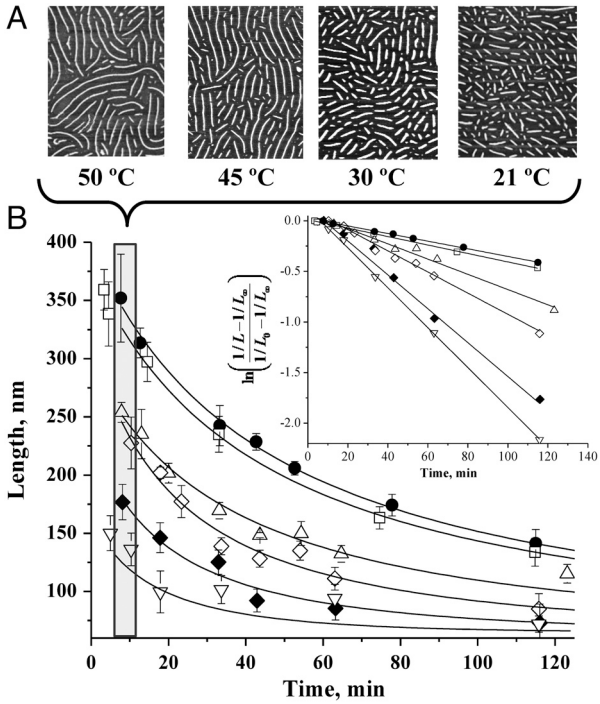

Fig. 2. (*A*) AFM height images of bottlebrush macromolecules on a mica substrate after spending 10 minutes on the surface of pure water at different temperatures. (*B*) Kinetics of the decrease of the average polymer chain length (*L*) on the water substrate at different temperatures (50 °C (●); 45 °C (□); 40 °C (△); 36 °C (◇); 30 °C (◆) 21 °C (▽)). Solid curves were obtained by fitting the experimental data points using Eq. **1**. (*Inset*) Plot of $\ln((1/L - 1/L_\infty)/(1/L_0 - 1/L_\infty))$ vs. time [Eq. **1**] at different temperatures. The slopes of the lines give the corresponding rate constants of the scission reaction.

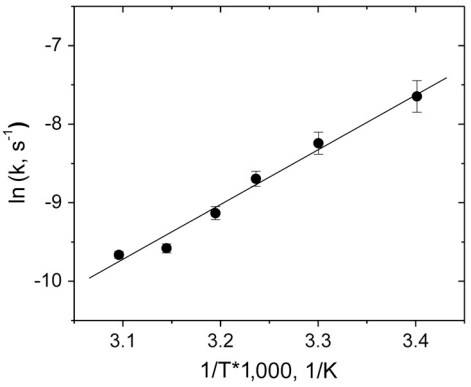

Fig. 3. The scission rate constant ($\ln k$) decreases with temperature. The data points (●) were obtained from the fitting analysis of the kinetic traces in Fig. 2 with Eq. **1** using k as a single fitting parameter. The solid line is a linear fit with $\ln k \sim B_1/T$ [Eq. **10**] and $B_1 = (6.1 \pm 0.4) \cdot 10^3$ K.

$$\frac{1/L - 1/L_\infty}{1/L_0 - 1/L_\infty} = e^{-kt}, \qquad [1]$$

where L_0 is the initial chain length at $t = 0$ and $L_\infty = 65 \pm 10$ nm is the chain length at $t = \infty$ (3). For each temperature dataset, the initial time ($t = 0$) was assigned to the first collected data point. The L_∞ was measured in two ways: (*i*) the average length at long times (days) and (*ii*) the length of a shortest molecule observed. Both approaches gave similar values within the range of 65 ± 10 nm. Eq. **1** was used to fit the experimental data points with the rate constant k as a single fitting parameter (Fig. 2*B*, *Inset*).The rate constants so obtained are plotted in Fig. 3 as a function of reciprocal temperature ($1/T$). The semi-log plot $\ln k(1/T)$ clearly demonstrates the anti-Arrhenius behavior as the rate constant decreases with temperature.

Complementary to the temperature experiments, we also measured the bond-scission rate constant as a function of bond tension at a constant room temperature of $T_0 = 298$ K (Fig. 4). As in our earlier experiments (3, 25), the backbone tension was varied by adding small (<1 wt%) fractions of 2-propanol to the water subphase, which reduces its surface energy. As shown previously (2), in the regime of strong adsorption ($S \sim k_B T$/monomer), the backbone tension in molecular bottlebrushes on a substrate depends on surface energy as:

$$f = Sd, \qquad [2]$$

where d is the width of the adsorbed bottlebrushes and $S = \gamma_{wg} - (\gamma_{wp} + \gamma_{pg})$ is the spreading parameter, representing the differ-

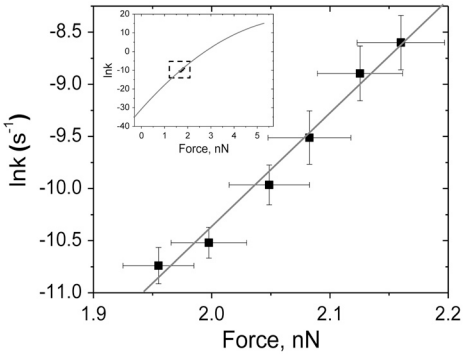

Fig. 4. The rate constant of the C—C bond scission reaction ($\ln k$) increases with tension in the brush backbone at room temperature $T_0 = 298$ K. Within a narrow interval of 1.9–2.2 nN, the $\ln k$ variation can be approximated using the linear function $\ln k \sim A_1 f$ [Eq. **9**] with $A_1 = 10.3 \pm 0.8$ nN^{-1}. (*Inset*) Within a broader range of bond tensions ($0 < f < f_m$), the logarithm of the rate constant ($\ln k$) exhibits nonlinear dependence on the tension.

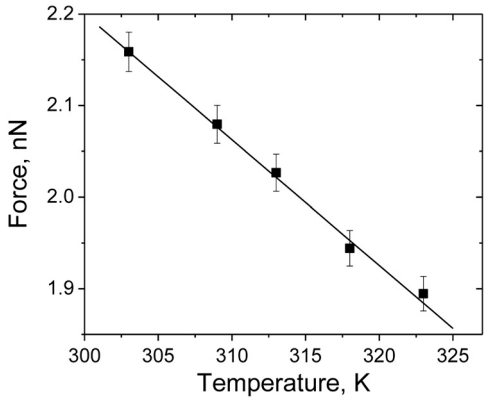

Fig. 5. The backbone tension in adsorbed bottlebrushes decreases with temperature due to the corresponding decrease of the spreading parameter [Eq. **2**], which was measured independently (*SI Text*). The solid line is a linear fit with Eq. **3**.

ence between the interfacial energies for water/gas (wg), water/polymer (wp), and polymer/gas (pg) interfaces. The brush width was determined as an average distance between worm-like macromolecules in atomic force microscopy (AFM) micrographs of Langmuir-Blodget monolayers prepared at a transfer ratio of 98%. The spreading parameter was independently measured through use of a Langmuir balance as a function of the propanol concentration and temperature (Figs. S1 and S2). On pure water at temperature $T = 303$ K, we have measured $d = 99 \pm 5$ nm and $S = 21.8 \pm 0.5$ mN/m, which give a backbone tension of $f = 2.16 \pm 0.13$ nN.The uncertainty in f reflects the standard deviation of d and S from their mean values measured for a set of 500 molecules and 10 isotherms, respectively.

To summarize the experimental findings, we have shown that temperature slows down the bond-scission reaction in adsorbed molecular brushes (Fig. 3). This behavior contrasts with the acceleration effect of mechanical force (Fig. 4). The negative temperature effect is ascribed to a decrease of the spreading parameter with temperature (Figs. S2 and S3), leading to the corresponding decrease of the backbone tension (Fig. 5). Within the studied temperature interval from $T = 303$ to 323 K ($\Delta T = 20$ K), the temperature effect on the backbone tension is approximated by a linear equation

$$f = a - bT, \qquad [3]$$

where $a = 6.3 \pm 0.2$ nN and $b = 0.0138 \pm 0.0008$ nN/K.

Data Analysis. ***Rate constant.*** Bond scission in the backbone of molecular bottlebrushes (Fig. 1) is an irreversible process because the bond recombination is hindered by steric repulsion of the side chains. By considering the force-induced bond scission as a thermally activated process, we can write down the rate constant as:

$$k = k_0 e^{-\frac{\Delta V}{k_B T}}, \qquad [4]$$

where $k_B = 1.38 \cdot 10^{23}$ J/K is the Boltzmann's constant and T is the Kelvin temperature of the reaction. The prefactor k_0 is assumed to be constant within the narrow interval of temperatures ($T = 303$–323 K) studied in this paper. The energy barrier $\Delta V = V(x_{TS}) - V(x_0)$ is the difference between the maximum and minimum of the bond potential, where x_0 and x_{TS} are reaction coordinates corresponding to the equilibrium and transition states, respectively (Fig. 6*B*). For a fully extended carbon chain under uniaxial tension, it is convenient to choose the reaction coordinate $x = r - r_0$ as a change of distance between the neighboring carbon atoms in the backbone along the force direction (Fig. 6*A*). In this case, the effective potential per repeat unit of the strained polymer chain can be written as:

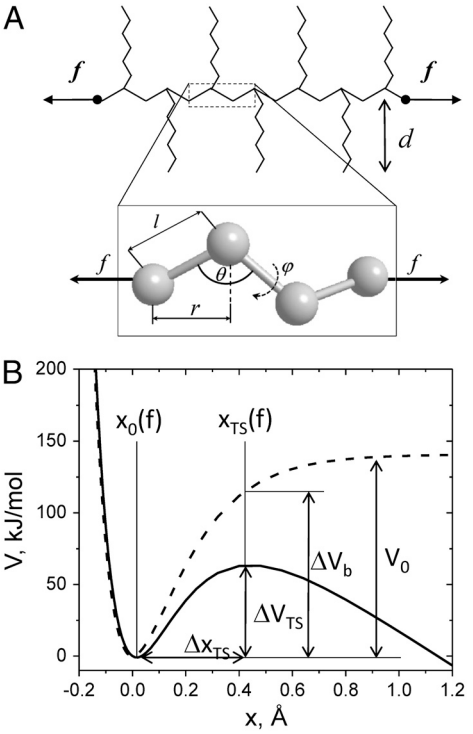

Fig. 6. Effective potential per repeat unit of a strained polymer chain (brush backbone) under uniaxial tension. (*A*) The reaction coordinate was chosen as $x = r - r_0$ along the force direction. (*B*) The potential was constructed using Eq. **5** with $V_0 = 141 \pm 19$ kJ/mol and $\beta^{-1} = 0.18 \pm 0.03$ Å, determined in this study. Both the height $\Delta V_{TS} = V(x_{TS}) - V(x_0)$ and length $\Delta x_{TS} = x_{TS} - x_0$ of the potential depend on bond tension, and $\Delta V_b(x_{TS})$ is the potential energy of an unperturbed bond at $x = x_{TS}$.

$$V = V_0(1 - e^{-\beta x})^2 - fx, \qquad [5]$$

where the first term $V_b = V_0(1 - e^{-\beta x})^2$ is a cumulative Morse potential, which integrates the potential energies of deformation of the bond length and angles (Fig. 6*A*). The parameters β^{-1} and V_0 determine the width and depth of the potential well, respectively. The second term corresponds to the mechanical work of the intramolecular force as $V_f = \int_0^x f(\xi)d\xi = fx$, facilitated by the well-defined magnitude and direction of the tensile force f. Indeed, bottlebrushes represent force-controlled tensile machines that generate constant force [Eq. **2**] directed along the backbone (Fig. 6*A*). Thermal fluctuations of the force orientation are negligible on length scales smaller than the brush width $d \sim 100$ nm, which determines the persistence length of bottlebrushes (26,27) exceeding several micrometers on substrates (1). It should also be noted that the backbone in adsorbed macromolecules is fully extended, adopting an *all-trans* conformation due to the nN-level tension (Fig. 1). This far exceeds the linear chain extension regime ($f \sim 1$ pN) and belongs to the so-called non-universal regime (28).

Activation barrier. By taking the derivative of Eq. **5** one finds two local extrema that yield the following relations for the height ΔV_{TS} and width Δx_{TS} of the activation energy barrier as a function of force:

$$\Delta V_{TS} = V_0\sqrt{1 - f/f_m} - f\Delta x \qquad [6]$$

and

$$\Delta x_{TS} = \frac{V_0}{2f_m} \ln \frac{1 + \sqrt{1 - f/f_m}}{1 - \sqrt{1 - f/f_m}}, \qquad [7]$$

where $f_m = (\partial V_b/\partial x)_{\max} = \beta V_0/2$ is the maximum bond tension. Note that substitution of Eq. **7** into Eq. **6** gives equation 16 in the 1940 Kauzmann-Eyring paper (4).

Fitting the experimental data. To fit the experimental data in Figs. 3 and 5, we represent the rate constant [Eq. **4**] in the logarithmic form as:

$$\ln k(f) = \ln k_0 - \frac{\Delta V(f)}{k_B T} \quad [8]$$

with the energy barrier $\Delta V(f)$ given by Eq. **6**. Because the measurements were conducted over a relatively narrow interval of forces, the experimental data points in Figs. 3 and 4 determine two local slopes of the functions $\ln k(1/T)$ and $\ln k(f)$, respectively. To analyze the slopes, the function in Eq. **8** was approximated by a Taylor series in a neighborhood of the mean force $f_a = 2.06$ nN and temperature $T_a = 313$ K. Due to the *ca.* 10% experimental error, it was sufficient to limit the Taylor approximation to its first order as:

$$\ln k \cong A_0 + A_1(f - f_a) \quad [9]$$

$$\ln k \cong B_0 + B_1(1/T - 1/T_a) \quad [10]$$

The coefficients A_1 and B_1, respectively, correspond to the first derivatives of Eq. **8** with respect to f and $1/T$, which can be calculated using Eqs. **3**, **6**, and **7** as:

$$A_1 \equiv \frac{\partial \ln k(f_a)}{\partial f} = -\frac{1}{k_B T}\frac{\partial \Delta V(f_a)}{\partial f} = \frac{\Delta x(f_a)}{(k_B T)} \quad [11]$$

$$B_1 \equiv \frac{\partial \ln k(T_a)}{\partial (1/T)} = \frac{1}{k_B}(b T_a \Delta x(T_a) - \Delta V(T_a)) \quad [12]$$

Note that the first derivative of the dissociation energy barrier $\Delta V(f)$ explicitly corresponds to the width of the activation barrier $\Delta x(f)$ at a given force f [Eq. **11**]. This validates the phenomenological approximation $\Delta V \cong E_a - fx$ by Zhurkov and Bell discussed in *Conclusions* (5, 6).

Eqs. **9** and **10** allow linear fitting of the experimental data points (Figs. 2 and 4) with the coefficients $A_1 = 10.3 \pm 0.8$ nN^{-1} and $B_1 = (6.1 \pm 0.4)10^3$ K determined by Eq. **11** and **12**. Note that we analyzed only local slopes within the ranges of temperature ($T = 303$–323 K) and bond tension ($f = 1.89$–2.16 nN) studied. No attempts were made to extrapolate the experimental data to zero f and $1/T$ because it would lead to largely inaccurate k_0 and V_0 values.

A solution of Eqs. **11** and **12** gives ΔV_{TS} and Δx_{TS}, which then can be substituted to Eqs. **6** and **7** to find the potential parameters, including the well depth V_0, maximum force f_m, well width $\beta^{-1} = V_0/(2f_m)$, and force constant $K_x = 2\beta^2 V_0$. Table 1 summarizes the results of these calculations. The determined maximum bond tension $f_m = 6.7 \pm 0.4$ nN is in agreement with the literature data (8). The barrier width $\Delta x_{TS} = 0.42 \pm 0.04$ Å is larger than the typically reported $\Delta l_{TS} \cong 0.35$ Å for homolytic scission of a C–C bond (29), which was expected due to contributions from the other molecular coordinates. Assuming that the most significant contributions in the fully extended *all-trans* polymer backbone result from the deformation of the bond length and bond angle, the barrier width can be estimated as $\Delta x_{TS} \cong \Delta l_{TS}\sin(\theta_0/2) + (\Delta\theta_{TS} l_0/2)\cos(\theta_0/2)$, where $l_0 = 1.54$ Å and $\theta_0 = 109°$ are the C–C bond length and the C–C–C bond angle. From $\Delta x_{TS} = 0.42$ Å and $\Delta l_{TS} = 0.35$ Å, this equation estimates the deformation of the bond angle at the transition state as $\Delta\theta_{TS} \cong 18°$.

The force constant $K_x = 1.45 \pm 0.36$ kN/m is markedly larger than the force constants of a C–C bond $K_l = 0.44$ kN/m reported for polymer chains (30, 31). The observed discrepancy is attributed to an additional potential due to deformation of the side chains that counteracts the deformation of the backbone. Rough estimation of the side-chain contribution can be made using the Gaussian approximation (2). The total free energy of a 2-D polymer brush per repeat unit of the backbone in a dry state at a spreading parameter of $S = 0$ can be written as $F = F_{bb} + F_{sc} \cong k_{bb} r^2/2 + k_{sc} d^2/2$ (see Fig. 6*A* for r and d). Assuming that the molecular area does not change upon extension (i.e., $rd = A$), the above equation can be written as $F \cong k_{bb} r^2/2 + k_{sc} A^2/(2r^2)$. Minimization of the free energy $\partial F/\partial d = 0$ gives the equilibrium length of the spacer $r_0 \cong \sqrt[4]{k_{sc} A^2/k_{bb}}$. The second derivative at the equilibrium distance $k = [\partial^2 F/\partial r^2]_{r=r_0}$ gives the force constant of the bottlebrush $k \cong 4k_{bb}$. More accurate calculations (the subject of future studies) depend on the molecular dimensions, surrounding medium, and degree of chain extension.

The obtained depth of the potential well $V_0 = 141 \pm 19$ kJ/mol is lower than the typical C–C bond dissociation energies $V_0 = 170$–371 kJ/mol from molecular dynamics and density functional theory (DFT) simulations (29–33), yet it is consistent with an experimental range of $V_0 = 40$–220 kJ/mol determined from pyrolysis and fracturing of polymers (17, 34). The broad variation of the dissociation energy reported is ascribed to variations in molecular mechanism and physical conditions of a bond-scission reaction. In our case, the energetics of the scission reactions within the bottlebrush macromolecules are affected by two major factors: (*i*) aqueous environment due to adsorption to a water substrate and (*ii*) conformational constraint of the backbone, which is covalently encapsulated into a shell of adsorbed side chains.

Table 1 also includes the prefactor k_0 obtained from Eq. **9**. Due to the narrow range of the studied forces and, hence, our inability to confidently perform either zero-or maximum-force extrapolation, the obtained prefactor $k_0 \approx 10^{7\pm2}$ s^{-1} is the least accurate, yet it is well below the nominal frequency of attempts $\nu_0 = k_B T/h \cong 10^{12}$ s^{-1}. The frequency of attempts could be significantly reduced due to both conformational and packing constraints of the backbone imposed by the bottlebrush architecture and dense adsorption to a substrate.

Conclusions

The spontaneous rupture of brush-like polymer C–C bonds on aqueous substrates shows a distinct anti-Arrhenius kinetic behavior that was analyzed using a modified Arrhenius equation, taking into account the effect of temperature on surface tension. As seen in Figs. 3 and 4, the temperature-induced variations in bond tension (Fig. 4) are large enough to cause significant changes in the rate constant (Fig. 3). We can conclude that heating the substrate results in a decrease of the scission rate constant due to a corresponding decrease of the substrate surface energy. This result directly supports the conclusion of our previous paper:

Table 2. Bond potential and activation parameters obtained by fitting experimental data points

ΔV_{TS} kJ/mol	Δx_{TS} Å	V_0 kJ/mol	f_m nN	β^{-1} Å	K_x kN/m	k_0 s^{-1}
65 ± 10	0.42 ± 0.04	141 ± 19	6.7 ± 0.4	0.18 ± 0.03	1.45 ± 0.36	$\sim 10^{7\pm2}$

This bond-cleavage reaction exhibits extremely high sensitivity to surface free energy.

In conclusion, we want to address the difference in the analysis of experimental data when using the physical and phenomenological approaches introduced by Eyring (4), Zhurkov (5), and Bell (6), respectively. In the first case, the energy barrier (Eq. **6** and Fig. 6) can be presented as:

$$\Delta V_{TS} = \Delta V_b - f\Delta x, \quad [13]$$

where both the barrier width $\Delta x = x_{TS} - x_0$ and the corresponding difference in the bond potential $\Delta V_b = V_b(x_{TS}) - V_b(x_0) = V_0\sqrt{1 - f/f_m}$ depend on force. In the second case, the barrier is introduced as:

$$\Delta V_{TS} = E_a - fx, \quad [14]$$

where the activation energy E_a and length x are assumed to be constant (i.e., independent of the applied force f). Both approaches are actively used in the current research (35, 36) and it would be instructive to discuss their relevance to the current study. Their applicability depends on the width of a force range and a relative force value f/f_m studied. For relatively narrow force and temperature intervals, the linear fits (Eqs. **11** and **12**) of the $\ln k(f)$ and $\ln k(T)$ data (Figs. 3 and 4) give the following relationships between the activation parameters in Eqs. **13** and **14**: $x \equiv \Delta x(f_a)$ and $E_a \equiv \Delta V_b(f_a)$. In other words, both approaches give identical values corresponding to the average force $f_a = 2.06$ nN. For a wider force interval, the use of **13** would be more appropriate. In many papers, E_a is interpreted as the bond energy (6), which is valid only for low forces ($f/f_m \ll 1$). In our experiments with $f/f_m \cong 0.3$, the E_a value determined from Eqs. **14** deviates from V_0 by a factor of $\sqrt{1 - f/f_m} \cong 0.84$, (i.e., by 16%), which is cautiously acceptable due to the experimental errors of 10–20%.

Materials and Methods

The brush-like macromolecules were synthesized using Atom Transfer Radical Polymerization (ATRP) by grafting PBA side chains from a poly(2-hydroxyethyl methacrylate) (PHEMA) macroinitiator (Fig. 1) (37–39). A combination of molecular characterization techniques (GPC, LS, gravimetry, and AFM) was employed to measure the number-average degrees of polymerization of the brush backbone and side chains as $N = 2150 \pm 100$ and $n = 140 \pm 5$, respectively. Due to the high grafting density (nearly every monomeric unit of the backbone bears a long side chain) (40), these molecular bottlebrushes adopt an extended conformation, which is readily imaged by AFM.

The polymers were adsorbed from a dilute solution in chloroform onto a surface of water/2-propanol mixtures (0–1 wt % of 2-propanol) in a Langmuir-Blodgett trough (KSV 5000) equipped with PTFE barriers and a Wilhemy plate balance. Mixing water (Milli-Q double-distilled, $\rho = 18.2$ MΩ) and 2-propanol (Aldrich, 99%) allowed accurate (±0.1 mN/m) control of the surface energy within a range of 69–71 mN/m. The measurements were conducted under controlled vapor pressure of propanol to prevent excessive evaporation and thus ensure the constant surface energy of the substrate. The temperature was controlled through circulation of a thermostated liquid around the trough and independently monitored by a set of thermocouples placed at the water surface. The accuracy of the temperature measurements was ±0.5 K.

To arrest the bond-scission process, polymer mono layers were compressed and transferred to freshly cleaved mica at a constant pressure of 0.5 mN/m. The samples were imaged in tapping-mode using a multimode AFM from Veeco equipped with a NanoScope III a controller and silicon cantilevers with resonance frequencies of about 160 kHz, spring constants of 5.0 N/m, and radii less than 10 nm. Computer software developed in-house was used for analysis of length distribution of the imaged macromolecules.

ACKNOWLEDGMENTS. We thank M. Rubinstein, A.V. Dobrynin, and E.B. Zhulina for very illuminating suggestions. We gratefully acknowledge funding from the National Science Foundation (DMR-0906985, DMR-0969301, DMR-1122483).

1. Sheiko SS, et al. (2006) Adsorption-induced scission of carbon-carbon bonds. *Nature* 440:191–194.
2. Panyukov S, et al. (2009) Tension amplification in molecular brushes in solutions and at substrates. *J Phys Chem B* 113:3750–3768.
3. Lebedeva NV, Sun FC, Lee HI, Matyjaszewski K, Sheiko SS (2008) Fatal adsorption of brush-like macromolecules: High sensitivity of C—C bond cleavage rates to substrate surface energy. *J Am Chem Soc* 130:4228–4229.
4. Kauzmann W, Eyring H (1940) The viscous flow of large molecules. *J Am Chem Soc* 62:3113–3118.
5. Zhurkov SN (1965) Kinetic concept of strength of solids. *Int J Fract Mech* 1:311–322.
6. Bell G (1978) Models for the specific adhesion of cells to cells. *Science* 200:618–627.
7. Evans E, Ritchie K (1999) Strength of a weak bond connecting flexible polymer chains. *Biophys J* 76:2439–2447.
8. Beyer MK, Clausen-Schaumann H (2005) Mechanochemistry: The mechanical activation of covalent bonds. *Chem Rev* 105:2921–2948.
9. Caruso M, et al. (2009) Mechanically-induced chemical changes in polymeric materials. *Chem Rev* 109:5755–5776.
10. Yang Q, et al. (2009) A molecular force probe. *Nat Nanotechnol* 4:302–306.
11. Lenhardt J, et al. (2010) Trapping a diradical transition state by mechanochemical polymer extension. *Science* 329:1057–1060.
12. Wallace MI, Ying L, Balasubramanian S, Klenerman D (2001) Non-Arrhenius kinetics for the loop closure of a DNA hairpin. *Proc Natl Acad Sci USA* 98:5584–5589.
13. Segawa S-I, Suguhara M (1984) Characterization of the transition state of lysozyme unfolding. I. Effect of protein-solvent interactions on the transition state. *Biopolymers* 23:2473–2488.
14. Oliveberg M, Tan Y-J, Fersht AR (1995) Negative activation enthalpies in the kinetics of protein folding. *Proc Natl Acad Sci USA* 92:8926–8929.
15. Munoz V, Thompson PA, Hofrichter J, Eaton WA (1997) Folding dynamics and mechanism of b-hairpin formation. *Nature* 390:196–200.
16. Davis JS, Epstein ND (2009) Mechanistic role of movement and strain sensitivity in muscle contraction. *Proc Natl Acad Sci USA* 106:6140–6145.
17. Odell JA, Muller AJ, Narh KA, Keller A (1990) Degradation of polymer solutions in extensional flows. *Macromolecules* 23:3092–3103.
18. Price GJ, Smith PF (1993) Ultrasonic degradation of polymer solutions: 2. The effect of temperature, ultrasound intensity and dissolved gases on polystyrene in toluene. *Polymer* 34:4111–4117.
19. Davies DM, Stringer EL (2003) Smart aqueous reaction medium. *Langmuir* 19:1927–1928.
20. Mehta AD, Rief M, Spudich JA, Smith DA, Simmons RM (1999) Single-molecule biomechanics with optical methods. *Science* 283:1689–1695.
21. Merkel R, Nassoy P, Leung A, Ritchie K, Evans E (1999) Energy landscapes of receptor-ligand bonds explored with dynamic force spectroscopy. *Nature* 397:50–53.
22. Greenleaf WJ, Woodside MT, Block SM (2007) High-resolution, single-molecule measurements of biomolecular motion. *Annu Rev Biophys Biomol Struct* 36:171–190.
23. Cecconi C, Shank EA, Bustamante C, Marqusee S (2005) Direct observation of the three-state folding of a single protein molecule. *Science* 309:2057–2060.
24. Dudko OK, Hummer G, Szabo A (2008) Theory, analysis, and interpretation of single-molecule force spectroscopy experiments. *Proc Natl Acad Sci USA* 105:15755–15760.
25. Li Y, et al. (2011) Molecular tensile machines: Intrinsic acceleration of disulfide reduction by dithiothreitol. *J Am Chem Soc* 133:17479–17484.
26. Fredrickson GH (1993) Surfactant-induced lyotropic behavior of flexible polymer solutions. *Macromolecules* 26:2825–2831.
27. Zhang B, Gröhn F, Pedersen JS, Fischer K, Schmidt M (2006) Conformation of cylindrical brushes in solution: Effect of side chain length. *Macromolecules* 39:8440–8450.
28. Morrison G, Hyeon C, Toan NM, Ha B-Y, Thirumalai D (2007) Stretching homopolymers. *Macromolecules* 40:7343–7353.
29. Beyer MK (2000) The mechanical strength of a covalent bond calculated by density functional theory. *J Chem Phys* 112:7307–7312.
30. Schachtschneider JH, Snyder RG (1963) Vibrational analysis of the *n*-paraffins 2. Normal co-ordinate calculations. *Spectrochim Acta* 19:117–168.
31. Treloar LRG (1960) Calculations of elastic moduli of polymer crystals: Polyethylene and Nylon 66. *Polymer* 1:95–103.
32. Nyden MR, Stoliarov SI, Westmoreland PR, Guo ZX, Jee C (2004) Applications of reactive molecular dynamics to the study of the thermal decomposition of polymers and nanoscale structures. *Mater Sci Eng A Struct Mater* 365:114–121.
33. Knyazev VD (2007) Effects of chain length on the rates of C—C bond dissociation in linear alkanes and polyethylene. *J Phys Chem A* 111:3875–3883.
34. Regel VR, Slutsker AI, Tomashevskii EE (1972) The kinetic nature of the strength of solids. *Sov Phys Usp* 15:45–65.
35. Hanke F, Kreutzer HJ (2006) Breaking bonds in the atomic force microscope: Theory and analysis. *Phys Rev E Stat Nonlin Soft Matter Phys* 74:031909.
36. Ainavarapu SRK, Wiita AP, Dougan L, Uggerud E, Fernandez JM (2008) Single-molecule force spectroscopy measurements of bond elongation during a bimolecular reaction. *J Am Chem Soc* 130:6479–6487.
37. Matyjaszewski K, Xia J (2001) Atom transfer radical polymerization. *Chem Rev* 101:2921–2990.
38. Sheiko SS, Sumerlin BS, Matyjaszewski K (2008) Cylindrical molecular brushes: Synthesis, characterization, and properties. *Prog Polym Sci* 33:759–785.
39. Matyjaszewski K, Tsarevsky NV (2009) Nanostructured functional materials prepared by atom transfer radical polymerization. *Nat Chem* 1:276–288.
40. Neugebauer D, Sumerlin BS, Matyjaszewski K, Goodhart B, Sheiko SS (2004) How dense are cylindrical brushes grafted from a multifunctional macroinitiator? *Polymer* 45:8173–8179.